

Effect of Silver Doping for Performance of CdS Solar Cell Prepared by Thermal Vacuum Evaporation

¹Suha A. Fadaam, ²Hiba M. Ali, ³Kawkab D. Salim and ²Sameer Atta. Makki

¹Ministry of Education, Directorate General for Education, Baghdad AL-Rusafa/1, Baghdad, Iraq

²College of Education for Pure Science-Ibn Al-Haitham, University of Baghdad, Baghdad, Iraq

³Department of Physics, College of Education for Pure Sciences, University of Tikrit, Tikrit, Iraq

Abstract: CdS thin films have been prepared by high vacuum thermal evaporation on glass and silicon substrates. Doping by silver with different ratios (2 and 4%) at substrate temperature (300 K). We studying structure properties by the measurement of X-ray diffraction and the microscope of force atomic. The estimated of crystallites size from X-ray diffraction for CdS, CdS:2% Ag and CdS:4% Ag. XRD measurement disclosed that the CdS, CdS:2% Ag and CdS:4% Ag were of cubic crystal structure. Affirm the microscopy of force atomic on nano-metric size for thin films. The microscopy of force atomic realization shows the rough surface. AFM investigations showed that the produced CdS, CdS:2% Ag and CdS:4% Ag, be the shape of particles on shape of a balls. Has been determined the band gap for (CdS, CdS:2% Ag and CdS:4% Ag) from optical properties and found (2.8, 2.61 and 2.41) eV, respectively. The examine of properties solar cell (CdS, CdS:2% Ag and CdS:4% Ag) by manufacture from heterojunction (CdS/Si).

Key words: Structure properties, optical properties, photoluminescence and solar cell, vacuum, band gap, crystallites

INTRODUCTION

Cadmium sulphide regarded from thin films promising materials for solar cell. The band gap of CdS equal to 2.4 eV, broad, so that, used as window materials with much semiconductors such CdTe (Dobson *et al.*, 2000), Cu₂S, InP (Frass and Ma, 1977) and CuInSe with 14-16% efficiency (Su and Choy, 2000). Because the high cost of this materials has been develop this studies towards particularly thin polycrystalline films and polycrystalline compound semiconductors. Cadmium sulphide CdS can be deposition by may different technology such as thermal deposition (Ashour *et al.*, 1995; Mahmoud *et al.*, 2000), Chemical Bath Deposition (CBD) (Oliva *et al.*, 2001), molecular beam epitaxy (Hofmann *et al.*, 1993) and spray chemically (Battisha *et al.*, 2002)

MATERIALS AND METHODS

Experimental work: The films Cadmium Sulphide (CdS) doped with silver were prohibited via. thermal vacuum evaporation using coating unit in vacuity around 1.5×10^{-4} mbar. A weight of fixed from material CdS 99.99% pure and put it material in boat from molybdenum, after evaporation

Cadmium Sulphide (CdS) thin films we take different ratio (2) and (4%) from this weight from silver. We used thermal diffusion method to doped Cadmium Sulphide (CdS) thin films with Silver, the rate of evaporation was $\approx 2.42 \text{ A}^\circ/\text{sec}$ and the film thickness it was ($500 \pm 10 \text{ nm}$). The substrate glass and silicon was placed directly top the source at space of almost 18 cm.

RESULTS AND DISCUSSION

The 300 K substrate temperature this temperature the deposition thin films CdS to obtained thin films of golden yellow coloured. Figure 1 shows the X-ray pattern for the film prepared at 300 K as the substrate temperature for (CdS pure, CdS:2% Ag and CdS:4% Ag).

From sherrer equation was calculated the average grain size for the thin films has been prepared which include the width of the X-ray diffraction line (Uplane and Pawar, 1983):

$$G_s = \frac{0.9\lambda}{\beta \cos(\theta)} \quad (1)$$

Where:

θ = The diffraction angle

λ = The wavelength of X-ray

β = The FWHM

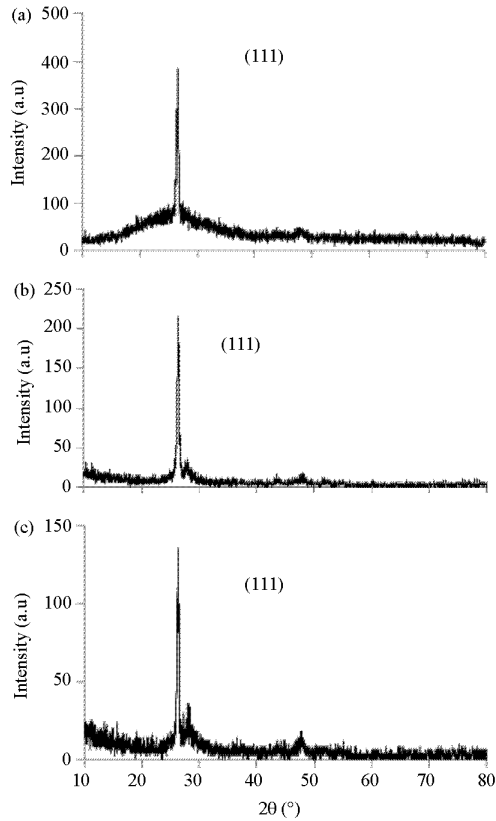


Fig. 1: XRD patterns of films deposited on glass substrate: a) CdS pure; b) CdS:2% Ag and c) CdS:4% Ag

Table 1: 2θ , G_s crystallite size, strain and dislocation density (CdS, CdS:2% Ag and CdS:4% Ag) thin films

Model	2θ (°)	(hkl)	G_s (nm)	$\eta \cdot 10^{-4}$ (lines $^{-2}$.m $^{-4}$)	$\delta \cdot 10^{14}$ (lines.m $^{-2}$)
CdS pure	26.565	111	25.679	14.692	15.164
CdS:2% Ag	26.362	111	22.806	16.543	19.224
CdS:4% Ag	26.346	111	22.316	16.906	20.078

The strain value (η) and the dislocation density (δ) value can be evaluated by using the relations in Eq. 2 and 3 (Lokhande, 1991) (Table 1):

$$\eta = \frac{\beta \cos(\theta)}{4} \quad (2)$$

$$\delta = \frac{1}{G_s} \quad (3)$$

Figure 2 shows the X-ray of Dispersed Energy (EDX) (supplement to system SEM) which used to know the internal element in the material composition. Noting in figure of emergence of peaks of the materials (Cd, S) and the appearance of other peak as impurities of matter (Ag).

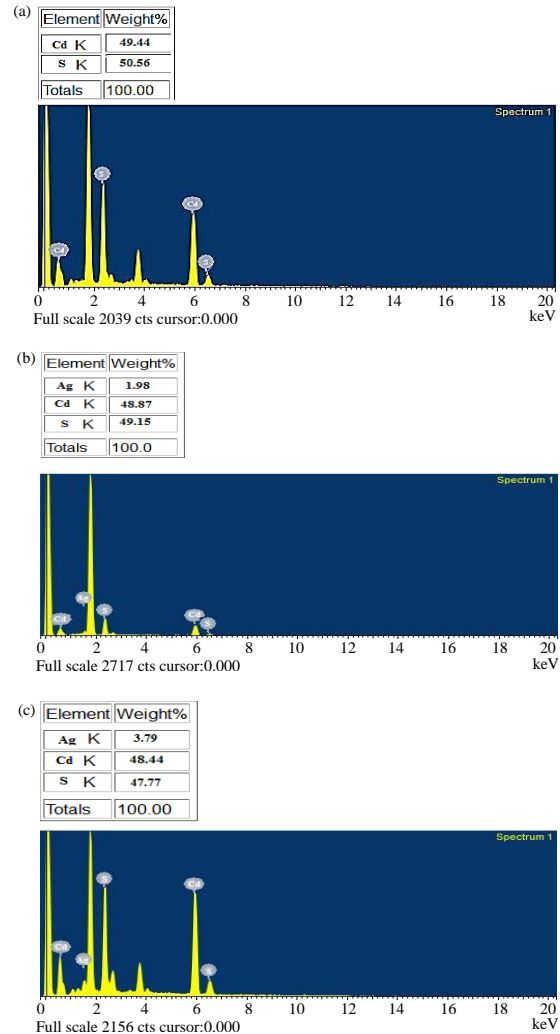


Fig. 2: EDX: a) CdS; b) CdS:2% Ag and c) CdS:4% Ag thin films

Table 2: Rate grain, roughness density and (RMS) of (CdS, CdS:2% Ag and CdS:4% Ag) thin films

Model	Avg. diameter (nm)	Roughness (nm)	Root mean
CdS pure	83.92	1.47	1.54
CdS:2% Ag	79.26	2.21	2.37
CdS:4% Ag	70.01	3.51	4.19

Figure 2 also shows a decrease in value of (S) due to reduction of material (S) and appearance of impurities (Ag) (Shehab and Fadaam, 2017).

Figure 3 exposes the (3-D) AFM image and split the graph of CdS, CdS:2% Ag and CdS:4% Ag, thin films on glass substrate. It is fully covered with CdS, CdS:2% Ag and CdS:4% Ag), diffuse of orderly on the surface. The value of roughness and the grain sizes are studied. It has been saw that a surface roughness and the grain size and the root mean square shows in Table 2. It is noted from

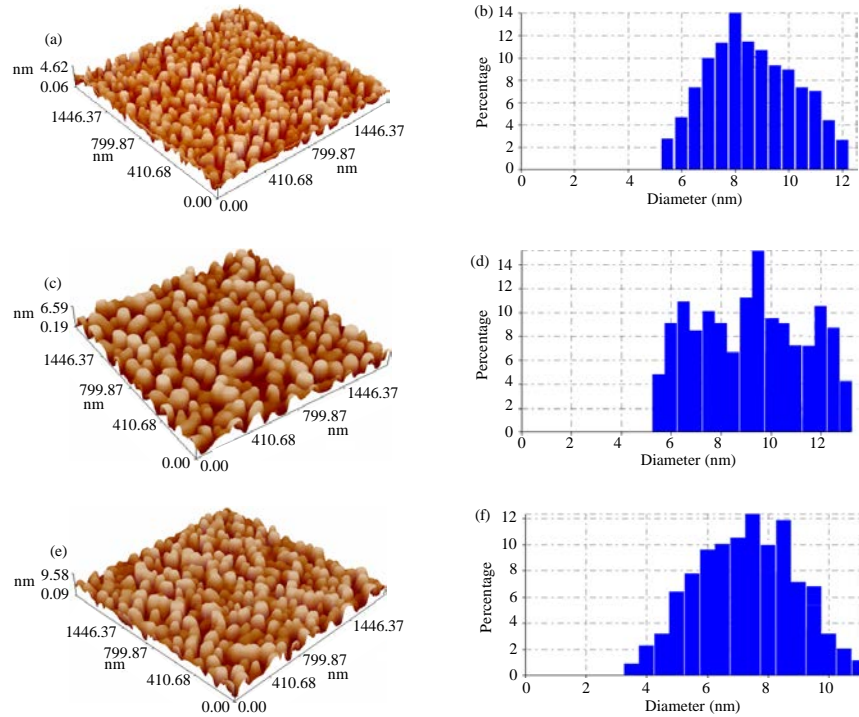


Fig. 3: 3-D AFM images and split the graph of thin films surface: a) CdS, c) CdS:2% Ag e) CdS: Ag 4% and b, d, f) Granulation cumulation distribution chart

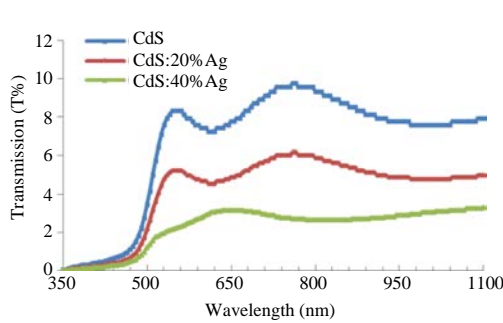


Fig. 4: Optical transmittance of (CdS pure, CdS:2% Ag and CdS:4% Ag) thin films

figure, decreases the grain size with increases ratio of impurities (Ag) and this is agreed with result of the X-ray diffraction.

Figure 4 shows Transmission (T) of (CdS pure, CdS:2% Ag and CdS:4% Ag) thin films that are prepared via. vacuum thermal evaporation and deposited on the substrate of glass. It is noticed from figure that the film CdS a gave the translucence of good at the rang of spectrum (300-1000) nm. Figure 4-8 transmission is increases pointedly due to the width of the absorbed partial size. The value of maximum transmission are (760.9, 760.6 and 760.2) nm for (CdSpre, CdS:2% Ag and CdS:4% Ag), respectively. The transmittance spectra show a

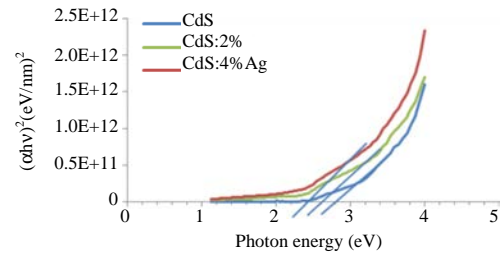


Fig. 5: Variation of energy gap for CdS: Ag films as a function of different doping ratio with silver

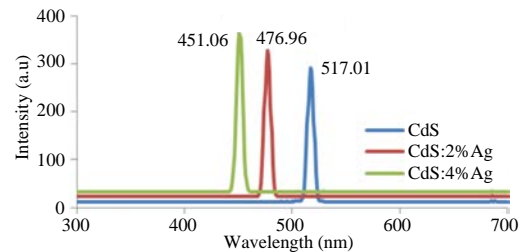


Fig. 6: PL spectra of CdS pure, CdS:2% Ag and CdS:4% Ag

decrease when increases the doping ratio of silver. Calculated the energy gap for CdS by the function (Lokhande *et al.*, 1998):

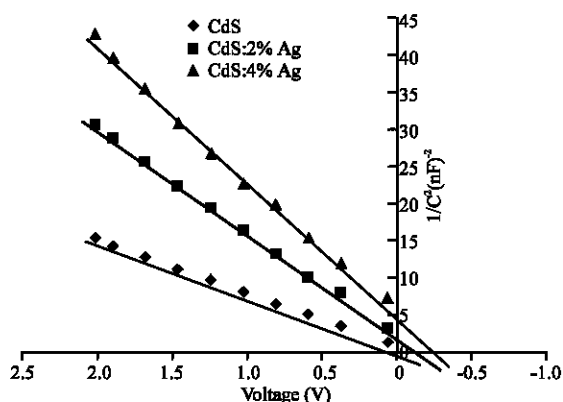


Fig. 7: $1/C_2$ versus reverse voltage of Al/CdS/P-Si/Al, Al/CdS:2% Ag/P-Si/Al and Al/CdS:4% Ag

Table 3:

Samples	V_{oc} (V)	I_{sc} (mA/cm ²)	P_m	F.F (%)	η (%)
CdS	2.23	0.38	0.506	59.8	2.93
CdS:2% Ag	2.82	0.74	1.356	65.06	3.18
CdS:4% Ag	4.21	0.89	3.088	82.40	4.04

$$\alpha h\nu = B(h\nu - E_g)^n \quad (4)$$

Figure 5 shows the band gap of thin films (CdS pure, CdS:2% Ag and CdS:4% Ag). The measurement of energy gap by draw the square $(\alpha h\nu)^2$ as function of photon energy by stabilizes the curve of the linear part towards the photon energy axis. The optical energy gap of (CdS, CdS:2% Ag and CdS:4% Ag) is found to be (2.8, 2.61 and 2.41) eV, respectively are decrease from incurrences doping ratios (Table 3).

Photo Luminescence (PL) use to determine of excitation wavelength for CdS thin films. Where the excitation wavelength source for this tin films was (451.06, 476.96 and 517.06) nm for (CdS, CdS:2% Ag and CdS:4% Ag), respectively as shown in Fig. 6. The excitation wavelength source compatible (451.06, 476.96 and 517.06) nm with energy gap obtained for the optical properties (Shehab *et al.*, 2018).

The linear relationship inverse of square of capacity ($1/C^2$) and reverse bias voltage for (CdS, CdS:2% Ag and CdS:4% Ag) indicated abrupt junction. The built-in potential V_{bi} value it was obtained after extrapolating the ($1/C^2$) point to the voltage axis. The V_{bi} it was (0.35, 0.27 and 0.15) volt but it was decreased with increases doping ratio with silver. For expected that value V_{bi} depend on the Fermi level position in the conduction band for CdS thin films.

Figure 8 shows the (1-5) curve under illumination where the photocurrent produced. The solar energy-to-

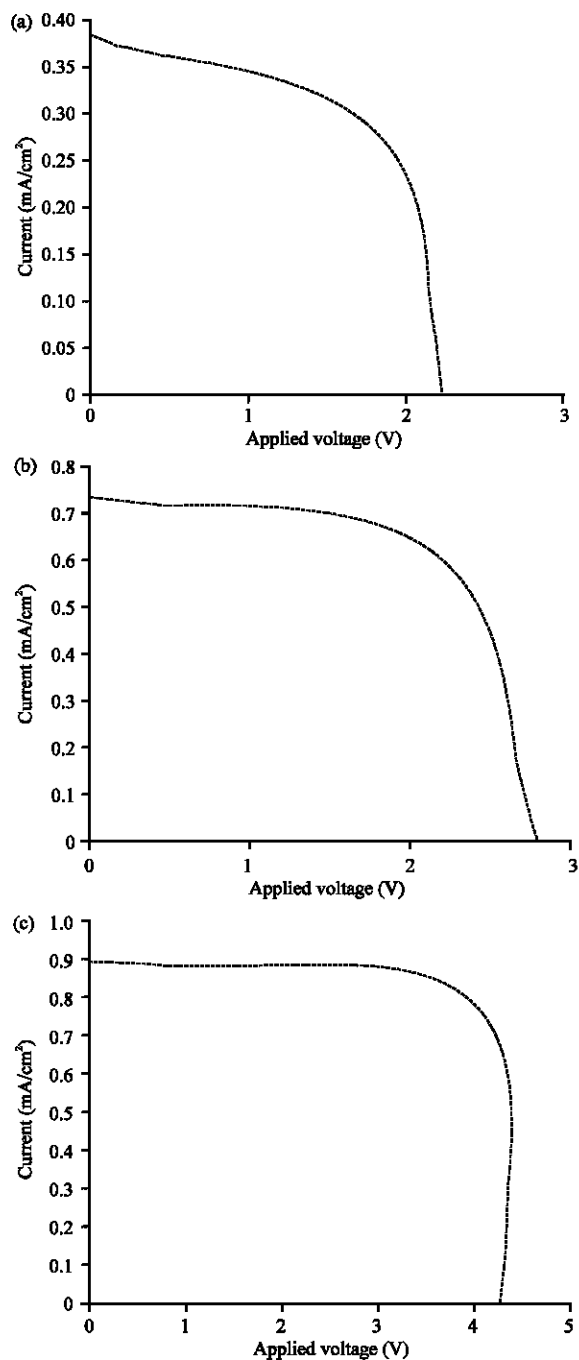


Fig. 8: a-c) 1-5 characteristics for Al/CdS/P-Si/Al, Al/CdS:2% Ag/P-Si/Al and Al/CdS:4% Ag

electricity conversion efficiency (η) was determined by Eq. 4, after calculating the following parameters, V_{oc} open circuit voltage, I_{sc} shortcircuit current density and F.F fill factor (Neamen, 2003). Table 3 shows, the value of efficiency the solar cell of Al/CdS/P-Si/Al, Al/CdS:2% Ag/P-Si/Al and Al/CdS:4% Ag:

$$\eta = \frac{P_m}{P_{in}} \times 100\% = \frac{I_m V_m}{P_{in}} \times 100\% \quad (4)$$

$$F.F = \frac{I_m V_m}{I_{sc} V_{oc}} \quad (5)$$

CONCLUSION

The cadmium sulphide was successfully prepared and then deposited as thin films by thermal evaporation method with different Ag ratios. From optical properties show that films could be helpful in photovoltaic solar cell applications. Performances for the CdS solar cell have been examined where the best results were recorded for J_{sc} , V_{oc} and η , for efficiency solar cell about 4.04, 4.04%.

REFERENCES

Ashour, A., N. El-Kadry and S.A. Mahmoud, 1995. On the electrical and optical properties of CdS films thermally deposited by a modified source. *Thin Solid Films*, 269: 117-120.

Battisha, I.K., H.H. Afify, G.A. El Fattah and Y. Badr, 2002. Raman and photoluminescence studies of pure and Sn-enriched thin films of CdS prepared by spray pyrolysis. *Fiz. ZAGREB*, 11: 31-42.

Dobson, K.D., I. Visoly-Fisher, G. Hodes and D. Cahen, 2000. Stability of CdTe/CdS thin-film solar cells. *Solar Energy Mater. Solar Cells*, 62: 295-325.

Fraas, L.M. and Y. Ma, 1977. CdS thin films for terrestrial solar cells. *J. Crystal Growth*, 39: 92-107.

Hofmann, P., K. Horn, A.M. Bradshaw, R.L. Johnson and D. Fuchs *et al.*, 1993. Dielectric function of cubic and hexagonal CdS in the vacuum ultraviolet region. *Phys. Rev.*, 47: 1639-1642.

Lokhande, C.D., 1991. Chemical deposition of metal chalcogenide thin films. *Mater. Chem. Phys.*, 27: 1-43.

Lokhande, C.D., A. Ennaoui, P.S. Patil, M. Giersig, M. Muller, K. Diesner and H. Tributsch, 1998. Process and characterisation of chemical bath deposited manganese sulphide (MnS) thin films. *Thin Solid Films*, 330: 70-75.

Mahmoud, S.A., A.A. Ibrahim and A.S. Riad, 2000. Physical properties of thermal coating CdS thin films using a modified evaporation source. *Thin Solid Films*, 372: 144-148.

Neamen, D., 2003. *Semiconductor Physics and Devices: Basic Principles*. McGraw Hill, New York, USA., ISBN:9780072321074, Pages: 746.

Oliva, A.I., O. Solys-Canto, R. Castro-Rodriguez and P. Quintana, 2001. Formation of the band gap energy on CdS thin films growth by two different techniques. *Thin Solid Films*, 391: 28-35.

Shehab, A.A. and S.A. Fadaam, 2017. Fabrication and study the characteristics of solar cell and detector optical Heterojunction type MnS/Si by Thermal Deposition. Ph.D Thesis, University of Baghdad, Baghdad, Iraq.

Shehab, A.A., S.A. Fadaam, A.N. Abd and M.H. Mustafa, 2018. Antibacterial activity of ternary semiconductor compounds AgInSe₂ nanoparticles synthesized by simple chemical method. *J. Phys. Confer. Ser.*, 1003: 1-11.

Su, B. and K.L. Choy, 2000. Electrostatic assisted aerosol jet deposition of CdS, CdSe and ZnS thin films. *Thin Solid Films*, 361: 102-106.

Uplane, M.D. and S.H. Pawar, 1983. Effect of substrate temperature on transport and optical properties of sprayed Cd_{1-x}Zn_xS films. *Solid State Commun.*, 46: 847-850.